Anisotropic band properties of the linear-chain nickelate Y_2BaNiO_5

L. F. Mattheiss
AT&T Bell Laboratories, Murray Hill, New Jersey 07974
(Received 11 March 1993)

The nonmagnetic band structure of Y_2BaNiO_5, an orthorhombic nickelate that contains one-dimensional (1D) chains of vertex-linked NiO_6 octahedra, has been calculated in the local-density approximation with the use of the linear augmented-plane-wave method. Neglecting magnetic effects, the results imply metallic behavior that originates from partially filled Ni($3d$) conduction bands with e_g character. This e_g manifold is composite in nature, featuring a relatively narrow ($\sim$0.3 eV) δ^*-type level amid a broader ($\sim$2 eV) σ^* subband with well-defined 1D characteristics. At half filling, for example, the components of the σ^*-band Fermi-velocity squared $\langle v_F^2 \rangle$ perpendicular to the chain axis are only $\sim$1–2 % of the corresponding parallel value. Although antiferromagnetism is expected to induce insulating behavior in this system, the present results may be relevant in doped systems if magnetism can be suppressed.

I. INTRODUCTION

The 1986 discovery of high-temperature superconductivity[1] in the layered perovskite-type compound $La_{2-x}Ba_xCuO_4$ has initiated ongoing efforts to synthesize new oxide phases that might also exhibit superconducting behavior. While several of these studies have led to the discovery of new superconducting cuprates, an equally important by-product of these investigations has been the identification of entirely new classes of transition-metal oxides as well as the discovery of new structure types. With this growing abundance of newly discovered transition-metal oxides, it is reasonable to expect that at least some of these "spin-off" materials will be found to possess physical properties that are equally as interesting as their superconducting counterparts.

Recently, Burdett and Mitchell[2] have investigated the electronic properties of a relatively new class of R_2BaMO_5 oxides with 2:1:1:5 stoichiometry in which R is a trivalent constituent (Y or a rare earth) and M is an appropriate transition element (M = Co, Ni, Cu, Zn, Pd, or Pt). Their analysis has focused on the 2:1:1:5 nickelates R_2BaNiO_5 which adopt an anisotropic orthorhombic structure with pronounced one-dimensional (1D) features. In particular, these 2:1:1:5 nickelates contain flattened NiO_6 octahedra that are vertex linked along one crystallographic axis but not in the basal plane. Actually, the best known member of this 2:1:1:5 family of transition-metal oxides is the so-called "green phase" cuprate Y_2BaCuO_5, which occurs[3] as an impurity in the synthesis of $YBa_2Cu_3O_7$. However, in contrast to the structural simplicity of the 1D 2:1:1:5 nickelates, this 2:1:1:5 cuprate adopts a more complex structure[4] that features isolated square-pyramidal CuO_5 clusters and Cu^{2+} ions at fivefold-coordinated sites.

The complete family of linear-chain 2:1:1:5 compounds is relatively large, containing a total of 15 members. While the linear-chain R_2BaMO_5 phases include a variety of lanthanides R, the transition-metal constituents are limited to M = Co or Ni. Based on an extended Hückel band calculation for the prototype compound Gd_2BaNiO_5, Burdett and Mitchell[2] have concluded that the Ni compounds are nonmagnetic semiconductors. According to their results, the Gd_2BaNiO_5 semiconducting properties originate from a $\sim$1-eV splitting within the Ni($3d$) e_g manifold in which the lower $d(x^2-y^2)$ states are filled and the upper $d(3z^2-r^2)$ subband is empty. This picture contradicts recent evidence[5] that at least some of the rare-earth R_2BaNiO_2 compounds are antiferromagnetic. For example, powder-neutron-diffraction studies[5] have shown that Er_2BaNiO_5 is antiferromagnetic below 33 K, with magnetic moments on both the Ni^{2+} and Er^{3+} sublattices. The corresponding data for Y_2BaNiO_5 are inconclusive. However, they are consistent with a model in which the Ni^{2+} moments are ordered antiferromagnetically along individual Ni-O-Ni chains but are uncorrelated on different chains.[5,6]

The purpose of the present investigation is to provide a more comprehensive understanding of the electronic properties of this family of linear-chain R_2BaNiO_5 compounds. To achieve this objective, a scalar-relativistic version[7] of the linear augmented-plane-wave (LAPW) method[8] has been applied to calculate the nonmagnetic band structure of Y_2BaNiO_5 in the local-density approximation (LDA).[9] Magnetic effects have been neglected here for several reasons. First, the nonmagnetic band-structure results are much simpler and thus more readily understood. Second, based on previous experience with the cuprates, it is anticipated that these nonmagnetic results may be relevant in doped systems if antiferromagnetism can be suppressed by altering the band filling via substitutional doping. Finally, the failure of local-spin-density calculations[10] to account for the insulating and antiferromagnetic properties of La_2CuO_4 has raised legitimate doubts concerning the adequacy of LDA results for describing the magnetic properties of cuprates and nickelates.

As is well known, low-dimensional materials have long

provided a special fascination for condensed-matter scientists. However, especially in the case of 1D systems, most theoretical studies have been based on highly simplified electronic-structure models. There have been relatively few instances where clearly identifiable 1D properties have emerged from the calculated results of an *ab initio* one-electron band-structure study. For example, although 1D behavior was proposed[11] several decades ago as a key ingredient for understanding the superconducting properties of the $A15$ compounds V_3Si and Nb_3Sn, such features were conspicuously absent in the band-structure results that were derived from subsequent first-principles calculations.[12]

Recently, my interest in 1D behavior and linear-chain compounds was revived by an analysis[13] of the band properties of CaNiN. This ternary nitride[14] contains NiN chains along the x and y axes which are separated by Ca layers. The calculated CaNiN band structure[15] exhibits a surprising feature whereby the σ^* (or σ-antibonding) bands are pushed below E_F, leaving conduction electrons with π^* rather than σ^* character. A detailed analysis has shown[13] that this σ^*-π^* reversal is due Ni $3d$-$4s$ hybridization effects. Presumably, such s-d hybridization effects are enhanced in CaNiN by the fact that Ni has only two N neighbors, which causes the effective Ni($4s$) orbital energy to be lowered in comparison to systems with higher coordination. While similar s-d hybridization effects are expected in the chain bands of the 1:2:3 superconductor $YBa_2Cu_3O_7$, they are diminished by the fourfold coordination at the chain-type Cu sites. Consequently, it is found that the σ^* band survives intact in this compound.[16] Thus a key objective of the present investigation is to determine the fate of the σ^* band in the linear-chain nickelate Y_2BaNiO_5, where each Ni is sixfold coordinated by oxygens.

II. COMPUTATIONAL DETAILS

The crystal structure of the R_2BaNiO_5 family of oxides was first described by Schiffler and Müller-Buschbaum[17] for the Nd compound Nd_2BaNiO_5. More recent x-ray-diffraction studies[18,19] have provided analogous structural information for the corresponding Y compound Y_2BaNiO_5. The present calculations have utilized the Y_2BaNiO_5 structural parameters that have been determined from single-crystal x-ray-diffraction studies by Buttrey, Sullivan, and Rheingold.[19] The specific values are listed in Table I. The small differences between the two independent Y_2BaNiO_5 structural determinations[18,19] are not expected to alter the essential features of the present LAPW results.

Y_2BaNiO_5 forms with a body-centered-orthorhombic structure that is illustrated in Fig. 1. The primitive cell contains one formula unit, and, for the purpose of the present calculations, the origin has been shifted so that a NiO_6 octahedron is centered at the origin. Neighboring NiO_6 octahedra share vertex oxygens [namely, those designated O(1) in Table I] to form linear chains along the c axis or z direction. These octahedra are compressed along the chains, and this leads to the presence of two short apical ($\sim$1.88 Å) and four long planar ($\sim$2.18 Å) Ni-O bond distances in this compound. As shown in Fig. 1, these vertex-linked octahedral chains are separated by intermediate Y and Ba cations. Based on previous experience with cuprates,[16] these constituents are expected to be chemically and electronically inactive in the nickelates. As shown by the results in the following section, they contribute minimal orbital weight to the band states near E_F. Their primary role is to provide structural and electronic isolation to the individual NiO_6 chains that make up the active electronic core of these materials.

TABLE I. Atom coordinates for the body-centered-orthorhombic nickelate Y_2BaNiO_5 with space group $Immm$ (D_{2h}^{25}) and lattice-parameter values $a=5.7760$ Å, $b=11.3581$ Å, and $c=3.7703$ Å, as determined by the x-ray-diffraction measurements of Buttrey, Sullivan, and Rheingold (Ref. 19). The present coordinates have been shifted and reoriented in order to place Ni at the origin and to align the vertex-linked NiO_6 octahedral chains along the z direction.

Atom	Type	x/a	y/b	z/c
Ba	$2d$	$\frac{1}{2}$	0	$\frac{1}{2}$
Y	$4h$	0	0.2061	$\frac{1}{2}$
Ni	$2a$	0	0	0
O(1)	$2c$	0	0	$\frac{1}{2}$
O(2)	$8h$	0.2394	0.1490	0

The Y_2BaNiO_5 phase exhibits the symmetry of the orthorhombic space group $Immm$ (D_{2h}^{25}), which is symmorphic and thus contains only primitive translations. The D_{2h} point group includes those eight symmetry operations[20] which send a rectangular solid into itself, regardless of the lengths of its sides. Because of orthorhombic symmetry, the NiO_6 octahedra in Y_2BaNiO_5 are not constrained to maintain their ideal shape. In fact, the distortions of these NiO_6 octahedra from the ideal square-planar geometry in the x-y plane are substantial. The positions of the orthorhombically distorted O(2)-type oxygens relative to the central Ni site in the Y_2BaNiO_5 basal plane are illustrated in Fig. 2. Here, the intracluster O(2)-O(2) bond lengths along the x and y directions are $\sim$2.77 and 3.38 Å, respectively. The shortest ($\sim$3.01 Å) intercluster O(2)-O(2) bonds, which occur along the x axis in Fig. 1, are intermediate in length. These represent the most likely path for interchain-coupling effects that will ultimately limit the 1D behavior of these materials.

The primitive lattice vectors for the body-centered-orthorhombic Bravais lattice can be written

$$\mathbf{t}_1=-\frac{a}{2}\hat{\mathbf{i}}+\frac{b}{2}\hat{\mathbf{j}}+\frac{c}{2}\hat{\mathbf{k}}\ ,$$
$$\mathbf{t}_2=+\frac{a}{2}\hat{\mathbf{i}}-\frac{b}{2}\hat{\mathbf{j}}+\frac{c}{2}\hat{\mathbf{k}}\ , \qquad (1)$$
$$\mathbf{t}_3=+\frac{a}{2}\hat{\mathbf{i}}+\frac{b}{2}\hat{\mathbf{j}}-\frac{c}{2}\hat{\mathbf{k}}\ ,$$

where the lattice-parameter values ($a=5.7760$ Å, $b=11.3581$ Å, and $c=3.7703$ Å) are those determined by Buttrey, Sullivan, and Rheingold.[19] The corresponding reciprocal-lattice vectors have the form

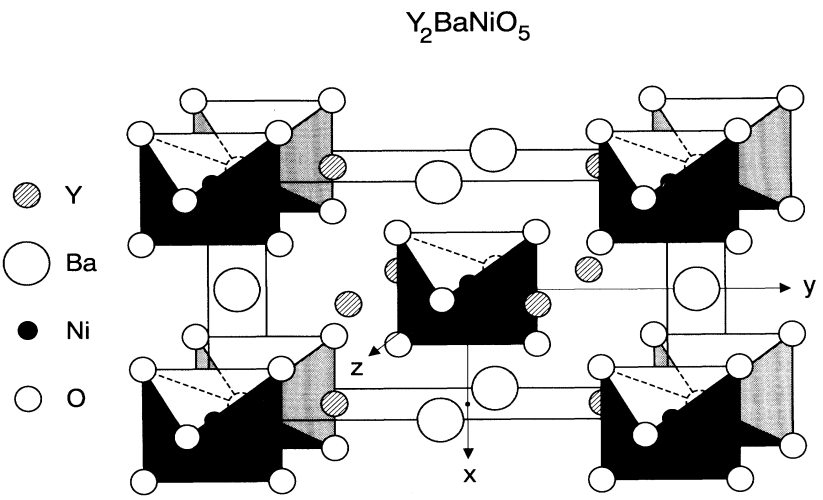

FIG. 1. A view of the nonprimitive body-centered-orthorhombic unit cell for Y_2BaNiO_5 which contains two formula units. The structure features vertex-linked NiO_6 octahedra that form well-defined chains along [001].

$$\mathbf{b}_1 = 2\pi(b^{-1}\hat{\mathbf{j}} + c^{-1}\hat{\mathbf{k}}) ,$$
$$\mathbf{b}_2 = 2\pi(a^{-1}\hat{\mathbf{i}} + c^{-1}\hat{\mathbf{k}}) , \quad (2)$$
$$\mathbf{b}_3 = 2\pi(a^{-1}\hat{\mathbf{i}} + b^{-1}\hat{\mathbf{j}}) .$$

These all-face-centered-orthorhombic vectors produce the Brillouin zone (BZ) that is shown in Fig. 3, where the main symmetry points and lines have been labeled in accordance with the notation of Cracknell *et al.*[20]

The present LAPW calculations utilize a full-potential implementation[7] which introduces no shape approximations in treating either the crystalline charge density or potential. Exchange and correlation effects have been introduced with the use of the Wigner interpolation formula.[21] The present study has used typical values for computational parameters and LAPW cutoffs. For example, the LAPW basis has included plane waves with a 12-Ry cutoff ($\sim$590 LAPW's), which is expected to yield bands that are converged in energy to the $\sim$0.2-eV range. The spherical-harmonic expansions of the LAPW wave functions within the muffin-tin spheres include terms through $l=8$ (Y,Ba), 6 (Ni), or 5 (O), depending on the size of the individual radii [namely, $R(\mathrm{Y}) \approx 1.33$ Å, $R(\mathrm{Ba}) \approx 1.44$ Å, $R(\mathrm{Ni}) \approx 1.01$ Å, and $R(\mathrm{O}) \approx 0.86$ Å, respectively].

In the present self-consistent calculation, the crystalline charge density and potential have been expanded using $\sim$5800 plane waves in the interstitial region and lattice-harmonic terms with $l_{\max}=4$ within the muffin-tin spheres. A 12-point **k** sample in the $\frac{1}{8}$ irreducible BZ wedge (which is outlined by the dashed lines in Fig. 3) has been used for calculating BZ averages. The Y($4d^1 5s^2$), Ba($5p^6 6s^2$), Ni($3d^9 4s^1$), and O($2s^2 2p^4$) states are treated as valence electrons in the present calculation while the remaining inner-shell states are included using a frozen-core approximation.[7]

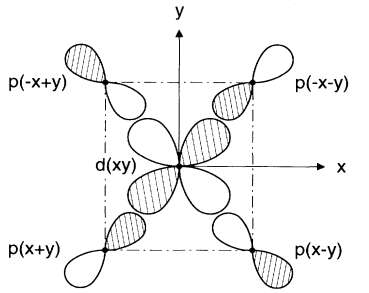

FIG. 2. A sketch illustrating the σ-bonding orbitals at the Ni and O(2) sites in the basal plane of the NiO_6 octahedra in Y_2BaNiO_5.

III. RESULTS AND DISCUSSION

The results of the present LAPW band-structure calculations for Y_2BaNiO_5 are plotted along selected symmetry lines in the body-centered-orthorhombic BZ in Fig. 4. The valence-band manifold contains a total of 20 bands, including 15 O($2p$)-derived states that occur at energies below -2 eV and the five Ni($3d$) bands that are clustered near E_F. Neglecting the corelike Ba($5p$) and O($2s$) levels, the unit cell contains a total of 38 valence electrons, so that two additional electrons are required to fill the

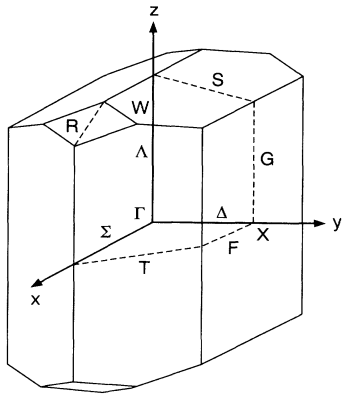

FIG. 3. The primitive Brillouin zone for the body-centered-orthorhombic lattice, with dimensions scaled in accordance with the Y_2BaNiO_5 lattice-parameter values in Table I. Symmetry labels follow the notation of Cracknell *et al.* (Ref. 20).

valence bands completely. A small (~ 0.3 eV) gap separates the Ni($3d$) and O($2p$) manifolds. Thus, in contrast to the cuprates where the Cu($3d$) and O($2p$) orbital energies are nearly degenerate and the corresponding bands are strongly admixed,[16,22] Y_2BaNiO_5 exhibits a small but well-defined energy gap that separates the O($2p$) and Ni($3d$) complexes. As shown by the results in the Appendix, a comparable gap is also present in the corresponding bands for the tetragonal 2D nickelate La_2NiO_4. An important consequence of this O($2p$)-Ni($3d$) energy separation is the fact that states near E_F in the nickelates will possess significantly less O($2p$) admixture than those in the cuprates. This is consistent with the Y_2BaNiO_5 density-of-states results that are presented below.

The Fermi level cuts through the midst of a composite e_g band that contains a relatively narrow (~ 0.3 eV) δ^* component as well as a broader (~ 2 eV) σ^* subband. The corresponding π^* bands, which overlap the σ^* bands in energy, remain below E_F and are completely filled. Thus, in regard to the e_g bands, the present LAPW results for Y_2BaNiO_5 differ fundamentally from those obtained previously in the extended-Hückel-theory study[2] where these two subbands are found to be separated by a ~ 1-eV gap, thus leading to the proposal that these linear-chain nickelates are nonmagnetic semiconductors. The unoccupied bands above ~ 1 eV in Fig. 4 represent some of the lower-lying Ba($5d$) and Y($4d$) states. In particular, the lowest band at the X symmetry point with energy ~ 1 eV corresponds to a Ba($5d$) state with predominant $d(3z^2-r^2)$ orbital symmetry along with some Y($4d$) admixture.

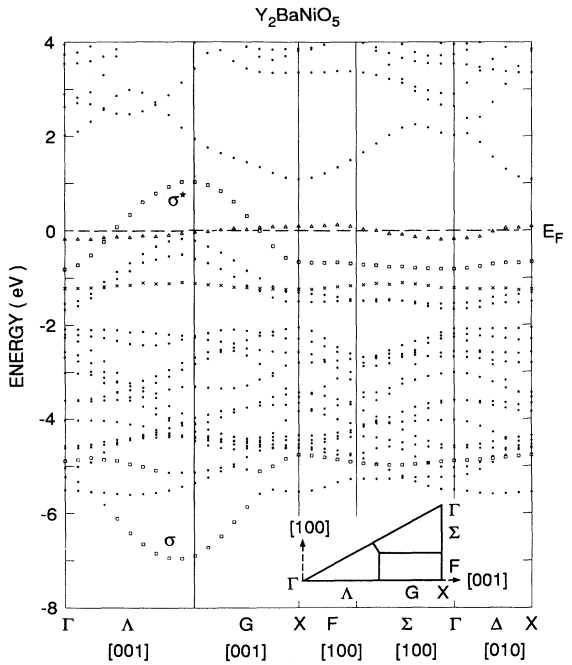

FIG. 4. LAPW energy bands for Y_2BaNiO_5 along select symmetry lines in the Brillouin zone, including directions with wave-vector components that are parallel (i.e., [001]) and perpendicular (namely, [100] and [010]) to the z-axis chains. The Λ-G and Σ-F lines are coplanar (see inset) in an extended-zone scheme. Bands with significant Ni $d(3z^2-r^2)$–O(1)$p(z)$, Ni $d(xy)$, and Ni $d(x^2-y^2)$ orbital weight ($w > 0.3$) within the corresponding muffin tins are identified by squares, triangles, and crosses, respectively. The remaining "background" bands are represented by filled dots.

The Y_2BaNiO_5 bands in Fig. 4 are plotted along the symmetry lines Λ, G, F, and Σ (which the inset shows are coplanar in an extended-zone scheme) as well as one perpendicular (Δ) direction. The Λ-G line is parallel to [001], the linear-chain direction. The bands labeled with the square symbols represent bonding (σ) and antibonding (σ^*) combinations of Ni $d(3z^2-r^2)$ and O(1) $p(z)$ orbitals. The flat component of the Ni e_g manifold has predominant $d(xy)$ character.[23] As shown in Fig. 2, this $d(xy)$ orbital forms σ-bonding molecular-orbital-type levels with appropriate combinations of O(2) $p(x)$ and $p(y)$ orbitals. However, since symmetry prevents interactions with apical-oxygen p orbitals, the resulting $d(xy)$ bandwidth is quite small (~ 0.3 eV). It originates from ($dd\delta$)-type interactions between Ni $d(xy)$ orbitals that are centered in adjoining NiO_6 octahedra. The lower-lying π^* subbands also exhibit dual character. Namely, this complex contains a relatively flat $d(x^2-y^2)$ component (which is identified by x's) along with a pair of more dispersive $d(xz)$-$d(yz)$ subbands that are labeled with filled dots.

The Ni $d(3z^2-r^2)$, $d(xz)$, and $d(yz)$ bands near E_F exhibit visible evidence for 1D behavior, dispersing when changes in the wave vector $\mathbf{k}$ include components along the chain axis, and remaining comparatively flat when only perpendicular components are varied. A further measure of 1D behavior is provided by the symmetry of the bands about the midpoint (which is one $\Delta\mathbf{k}$ unit to the left of the vertical line) of the Λ-G direction since, in the primitive BZ of Fig. 3, these represent two parallel lines that are separated by half the BZ width, $\Delta k_y = 2\pi/b$. Further evidence of 1D character is provided by the LAPW results along two additional [001] BZ lines that are shown in Fig. 5. These results, which involve intermediate values of $k_y = \pi/b$, are rigorously symmetric about their midpoints in an extended-zone scheme. Overall, the combined results in Figs. 4 and 5 provide consistent evidence for the presence of 1D band characteristics in Y_2BaNiO_5.

The results shown in the right-hand panel of Fig. 5(c) have been derived from a nine-parameter tight-binding (TB) model that is designed to mimic the LAPW valence-band results for Y_2BaNiO_5. These TB parameters, which are listed in Table II, include only intracluster O($2p$)-Ni($3d$) interactions. Among these TB parameters, there is a Ni($3d$) orbital energy ε_d, pairs of crystal-field split O(1) and O(2) $\varepsilon_{p\sigma}$ and $\varepsilon_{p\pi}$ levels, and two sets of nearest-neighbor NiO ($pd\sigma$) and ($pd\pi$) interaction parameters. As a consequence of vertex linking, the former interactions [i.e., those involving Ni-O(1)] produce 1D dispersion along the chains. On the other hand, the Ni-O(2) interactions lead to the formation of molecular-orbital-type levels but add no dispersion. It is clear from Fig. 5(c) that this purely 1D TB model provides a qualita-

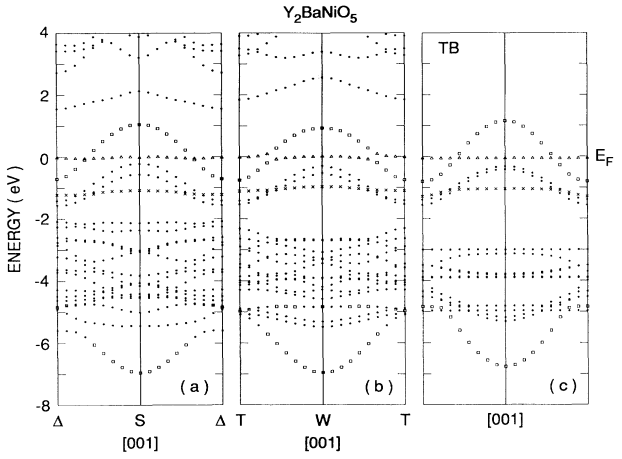

FIG. 5. A comparison of LAPW bands for Y_2BaNiO_5 along two independent [001] Brillouin-zone directions [(a) and (b), respectively] with those derived from a simple tight-binding (TB) model (c). The LAPW results, which have $k_y=\pi/b$, are symmetric about their midpoints S and W, respectively, and are coplanar in an extended-zone representation. Band labels continue the notation of Fig. 4.

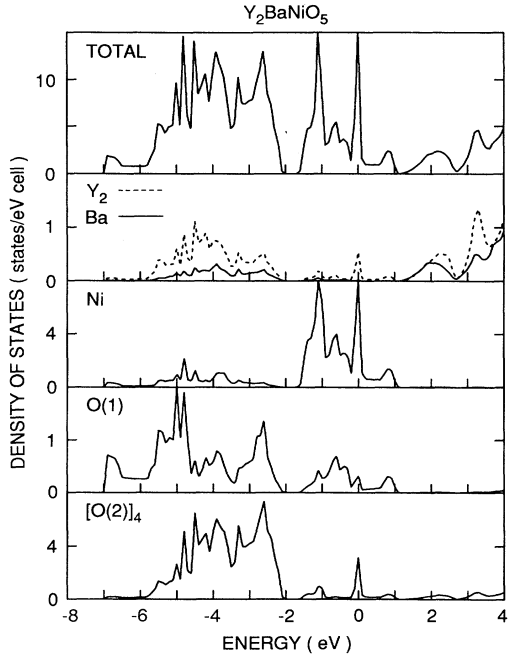

FIG. 6. Total and muffin-tin-projected density-of-states results for Y_2BaNiO_5.

tive representation of the LAPW conduction-band results for Y_2BaNiO_5. Comparing TB parameters for the nickelates and cuprates,[22] the main difference centers on ε_d, which results from the increased binding energy of the Cu($3d$) versus Ni($3d$) levels. Thus, while $\varepsilon_p \approx \varepsilon_d$ in the cuprates, this degeneracy is removed in the nickelates, where $\varepsilon_p < \varepsilon_d$.

An overview of the Y_2BaNiO_5 electronic properties is provided by the density-of-states (DOS) curves that are shown in Fig. 6. These DOS results have been calculated with the use of tetrahedral interpolation[24] based on LAPW bands at 36 uniformly distributed **k** points in the irreducible $\frac{1}{8}$ BZ. Unlike the corresponding results[16,22] for typical cuprate superconductors such as $La_{2-x}Ba_xCuO_4$ or $YBa_2Cu_3O_7$, where the Cu($3d$) and O($2p$) bands are degenerate and strongly admixed, the Y_2BaNiO_5 DOS results emphasize the predominance of Ni($3d$) character in the split-off five-band complex near E_F. Similarly, the corresponding valence-band states at lower energies exhibit enhanced O($2p$) components in both the projected O(1) and $[O(2)]_4$ DOS results. As in the cuprates, Y_2 and Ba are basically ionic donor constituents (i.e., Y^{3+} and Ba^{2+}, respectively) that contribute minimal orbital weight to the DOS in the occupied valence-band region.

According to the DOS results in Fig. 6, the Y_2BaNiO_5 Fermi level occurs near the center of a sharp DOS peak that originates from the $d(xy)$-type δ^* subband. In order to fill or empty this peak via chemical doping, one must either add or subtract about one valence electron per formula unit. Adding one electron raises E_F by ~ 0.35 eV, reduces the value of the DOS at E_F to ~ 0.95 states/eV Ni, and leads to a situation where the σ^* band is exactly half filled. As emphasized previously,[13,16,22] this is an important band characteristic that is shared by the "parent compounds" of all known cuprate and bismuthate high-T_c superconductors. Thus substitutional doping of trivalent constituents for Ba (for example, La→Ba) should be explored in this system in efforts to induce metallic (and possibly superconducting) behavior in this system.

A simple extension of the tetrahedral DOS procedures permits one to calculate the average Fermi velocity. In the present investigation, this technique has been applied to calculate the average over the Fermi surface of the rms velocity components $\langle v_i^2\rangle^{1/2}$, where $\langle v_F^2\rangle = \langle v_x^2\rangle + \langle v_y^2\rangle + \langle v_z^2\rangle$. These results, which are shown in Fig. 7, provide a more quantitative measure of 1D effects in the electronic properties of Y_2BaNiO_5. It is clear from these results that the Y_2BaNiO_5 bands exhibit well-defined 1D

TABLE II. Tight-binding parameters for Y_2BaNiO_5. For the apical O(1) oxygens, the orbital energies $\varepsilon_{p\sigma}$ and $\varepsilon_{p\pi}$ represent $p(z)$ and $p(x)$-$p(y)$ orbitals, respectively. An analogous notation [i.e., $\sigma \equiv p(x+y)$; $\pi \equiv p(x-y)-p(z)$, etc.] identifies the corresponding σ- and π-type p-orbital energies for the planar O(2) oxygens.

Site	Parameter	Value (eV)
Ni	ε_d	−2.0
O(1)	$\varepsilon_{p\sigma}$	−3.5
	$\varepsilon_{p\pi}$	−3.7
O(2)	$\varepsilon_{p\sigma}$	−3.0
	$\varepsilon_{p\pi}$	−3.9
Ni-O(1)	$(pd\sigma)_1$	−1.8
	$(pd\pi)_1$	1.0
Ni-O(2)	$(pd\sigma)_2$	−1.4
	$(pd\pi)_2$	0.8

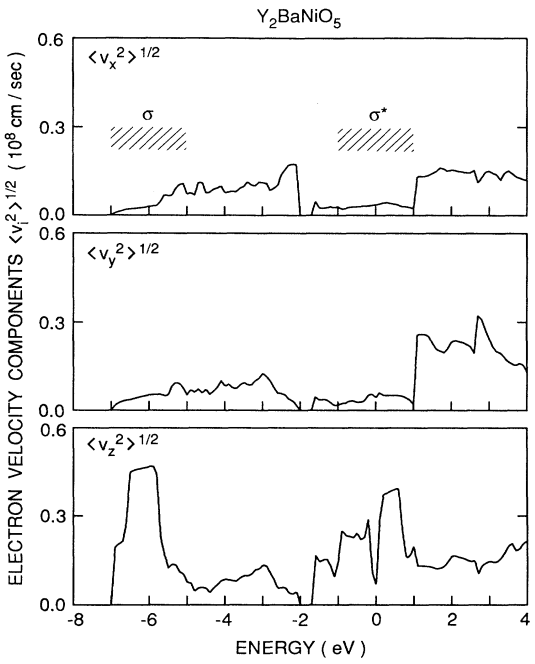

FIG. 7. The variation with energy of the calculated rms Fermi-velocity components $\langle v_i^2\rangle^{1/2}$ for Y_2BaNiO_5, where the average $\langle v_F^2\rangle$ is given by $\langle v_F^2\rangle=\langle v_x^2\rangle+\langle v_y^2\rangle+\langle v_z^2\rangle$. Crosshatching highlights the energy ranges where the 1D behavior of the σ-σ^* bands is prominent.

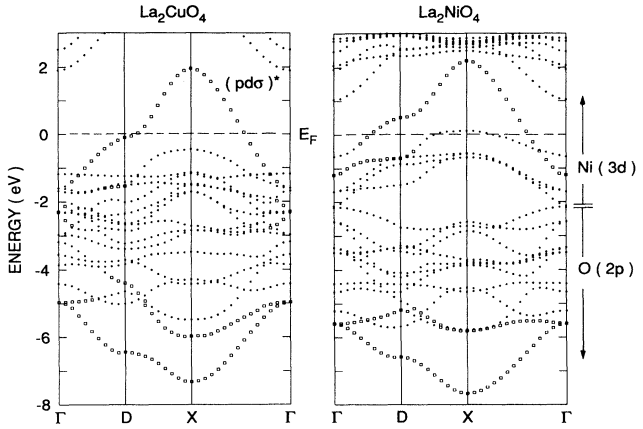

FIG. 8. A comparison of LAPW energy-band results for the layered K_2NiF_4-type phases of La_2CuO_4 and La_2NiO_4, where $D=(\pi/a,0,0)$ and $X=(\pi/a,\pi/a,0)$ in the body-centered-tetragonal Brillouin zone. Bands with significant $(pd\sigma)$ orbital character ($w>0.3$) are identified by square symbols, following the notation of Fig. 4.

characteristics in the energy range that is spanned by the σ and σ^* bands. However, these 1D features are washed out over the remainder of the valence-band energy range where the calculated velocity components are found to be more isotropic. It is noted that these 1D characteristics are diminished at the Y_2BaNiO_5 Fermi level by the presence of the narrow δ^* band.

In summary, the results of nonmagnetic band calculations for the orthorhombic linear-chain nickelate Y_2BaNiO_5 predict metallic behavior that originates from a half-filled e_g conduction band with narrow ($\sim$0.3 eV) and broad ($\sim$2 eV) components. In contrast to previous extended Hückel-theory results,[2] where these e_g subbands are split by crystal-field effects to produce a $\sim$1-eV semiconductor gap, the present results exhibit overlapping e_g components, thereby implying that the observed Y_2BaNiO_5 semiconducting behavior must originate from magnetic effects. The present results suggest that substitutional doping should be explored in Y_2BaNiO_5 to determine whether emptying or filling the DOS peak at E_F could possibly inhibit antiferromagnetism and thus induce 1D metallic behavior in this system.

ACKNOWLEDGMENTS

I am grateful to S.-W. Cheong for bringing the Y_2BaNiO_5 system to my attention, and for helpful discussions. I have also benefited from valuable conversations with A. P. Ramirez and J. Zaanen concerning the magnetic properties of Y_2BaNiO_5.

APPENDIX

The results of previous nonmagnetic band calculations[25,26] for the 2:1:4 layered perovskite La_2NiO_4 disagree as to whether the Ni($3d$) and O($2p$) bands overlap in this nearly 2D system. In both studies, computational methods that introduce shape approximations in treating the crystalline charge density and potential have been utilized. In particular, a linear muffin-tin-orbital calculation (atomic-sphere approximation) has predicted[25] an 0.8-eV gap between the O($2p$) and Ni($3d$) bands, while the results of an augmented-plane-wave calculation (muffin-tin approximation) exhibit significant ($\sim$1 eV) O($2p$)-Ni($3d$) band overlap.[26] To help resolve this issue, a full-potential LAPW calculation has been carried out for nonmagnetic La_2NiO_4 using structural parameters[27] that differ only slightly from those involved in the earlier studies.[25,26] These LAPW results for the 2:1:4 nickelate La_2NiO_4 are shown in Fig. 8, where they are compared with the corresponding bands[22] for the 2:1:4 cuprate La_2CuO_4. As shown in the right-hand panel, the present LAPW results for La_2NiO_4 reflect, in a sense, a crude average of the earlier results, exhibiting a tiny ($\sim$0.05 eV) gap between the O($2p$) and Ni($3d$) complexes. Thus, neglecting magnetic effects, both the 1D (i.e., Y_2BaNiO_5) and 2D (i.e., La_2NiO_4) nickelates are found to possess low-lying O($2p$) bands that are separated by a small energy gap from the Ni($3d$) states near E_F.

[1]J. G. Bednorz and K. A. Müller, Z. Phys. B **64**, 189 (1986).
[2]J. K. Burdett and J. F. Mitchell, J. Am. Chem. Soc. **112**, 6571 (1990).
[3]R. M. Hazen *et al.*, Phys. Rev. B **35**, 7238 (1987).
[4]C. Michel and B. Raveau, J. Solid State Chem. **43**, 73 (1982).
[5]J. A. Alonso, J. Amador, J. L. Martinez, I. Rasines, J. Rodriguez-Carvajal, and R. Saez-Puche, Solid State Commun. **76**, 467 (1990).
[6]S.-W. Cheong *et al.* (unpublished).
[7]L. F. Mattheiss and D. R. Hamann, Phys. Rev. B **33**, 823 (1986).
[8]O. K. Andersen, Phys. Rev. B **12**, 3060 (1975).
[9]P. Hohenberg and W. Kohn, Phys. Rev. **136**, B864 (1964); W. Kohn and L. J. Sham, *ibid.* **140**, A1133 (1965).
[10]T. C. Leung, X. W. Wang, and B. N. Harmon, Phys. Rev. B **37**, 384 (1988).
[11]M. Weger, Rev. Mod. Phys. **36**, 175 (1964); J. Labbé and J. Friedel, J. Phys. Radium **27**, 153 (1966).
[12]L. F. Mattheiss, Phys. Rev. **138**, A112 (1965); B. M. Klien, L. L. Boyer, D. A. Papaconstantopoulos, and L. F. Mattheiss, Phys. Rev. B **18**, 6411 (1978).
[13]L. F. Mattheiss, Phys. Rev. B **47**, 8224 (1993).
[14]M. Y. Chern and F. J. DiSalvo, J. Solid State Chem. **88**, 459 (1990).
[15]S. Massidda, W. E. Pickett, and M. Posternak, Phys. Rev. B **44**, 1258 (1991).
[16]L. F. Mattheiss and D. R. Hamann, Solid State Commun. **63**, 395 (1987).
[17]S. Schiffler and Hk. Müller-Buschbaum, Z. Anorg. Allg. Chem. **532**, 10 (1986).
[18]J. Amador *et al.*, Phys. Rev. B **42**, 7918 (1990).
[19]D. J. Buttrey, J. D. Sullivan, and A. L. Rheingold, J. Solid State Chem. **88**, 291 (1990).
[20]A. P. Cracknell, B. L. Davies, S. C. Miller, and W. F. Love, *Kronecker Product Tables* (Plenum, New York, 1979), Vol. I.
[21]E. Wigner, Phys. Rev. **46**, 1002 (1934).
[22]L. F. Mattheiss, Phys. Rev. Lett. **58**, 1028 (1987).
[23]The e_g symmetry of the $d(xy)$ orbital in Fig. 2 is due to the fact that coordinate axes are rotated about z by an angle $\phi=45°$ from that of the standard octahedral geometry, which is adopted by Burdett and Mitchell (Ref. 2).
[24]O. Jepsen and O. K. Andersen, Solid State Commun. **9**, 1763 (1971); G. Lehmann and M. Taut, Phys. Status Solidi B **54**, 469 (1972).
[25]G. Y. Guo and W. M. Temmerman, J. Phys. C **21**, L803 (1988).
[26]K. Takegahara and T. Kasuya, Solid State Commun. **70**, 641 (1989).
[27]B. Grande and Hk. Müller-Buschbaum, Z. Anor. Allg. Chem. **453**, 152 (1977).